CONFORMAL DUAL-BAND HIGH-FREQUENCY RADAR ANTENNA SYSTEM DESIGN FOR IMPLEMENTATION ON A SMALL UNMANNED AERIAL SYSTEM

Austin Feathers *(University of Kansas)*
Dr. Stephen Yan, Dr. Fernando Rodriguez-Morales, Dr. Richard Hale, Ali Mahmood, Katie Constant
CReSIS, University of Kansas
Lawrence, KS, U.S.A.
afeathers1@gmail.com

***Abstract*— High-frequency synthetic aperture radar (HF SAR) soundings from an aerial platform provide an effective method for sensing ice sheet basal topography. However, large manned aircraft are expensive to operate, introduce risk to the crew, and increase the risk of pilot error in sounding measurements. As well, the antennas associated with these HF/VHF soundings are too large to practically implement beneath large aircraft with conductive skins. Small unmanned aerial systems provide safe, inexpensive, and electrically unobstructive platforms for this radar equipment, necessitating the development of electrically small wide-band HF/VHF antenna systems that may be implemented conformally to the structure of such an aircraft. Conformity would help avoid affecting the platform's aerodynamic properties, and would reduce the potential for mid-flight variations in antenna geometry. Metallization of the non-conductive aircraft surface will be used to produce the antenna elements.**

The aircraft in question is the G1X-B, a 40% scale variant of the Yak-54 aerobatic aircraft, developed by the Aerospace Engineering department at the University of Kansas. Extended fiberglass wings in development will provide a 5.3 meter wingspan, increasing the surface available for metallization to produce the antenna. The HF and VHF frequencies being considered for dual-band operation are 14 MHz and 35 MHz respectively, as these exhibit high performance in ice-thickness sensing applications.

An antenna design which met directivity, bandwidth, and dual-band requirements, and which could be implemented conformally to the surface of the aircraft was finalized using simulation. It was then confirmed that a matching network could be used to tune the antenna and exceed bandwidth requirements. A scale model of the antenna was produced, in order to test production methods, and evaluate the performance of the model, compared to simulated results.

Key Words – SAR, Directivity, Surface-Conformal Implementation, Impedance Bandwidth, Dual-Band, G1X UAS (Previous), G1X-B UAS

I. INTRODUCTION

A. SAR

Synthetic Aperture Radar (SAR) is a signal processing technique used extensively for aerial or satellite topographical measurements. The technique uses multiple radar soundings from a small antenna, which is moving relative to the subject, to digitally construct (synthesize) an extremely large antenna aperture. This simulates the achievable resolution of an antenna of impractical proportions. The synthetic aperture allows for much finer resolution imagery than is capable with the antenna used to collect the soundings alone. This technique is employed extensively by CReSIS, using aerial antenna platforms. [1]

B. HF/VHF SAR soundings

Ice thickness is difficult to measure in fast-flowing glaciers or near calving-fronts. Surface features, as well as fractures and inclusions in the ice can cause scattering of the incident radiation, and cluttering of synthesized radar images collected using soundings at higher frequencies. Frequencies below 50 MHz (primarily HF and VHF), are useful for these measurements because they are not scattered as severely by smaller inclusions and inconsistencies in the ice. [1]

Of particular interest to CReSIS for this application are the bands of 14 MHz and 35 MHz, as they have been investigated, and perform favorably. [1] Unfortunately, antennas operating at these frequencies are not practical to implement underneath the large aircraft operated by CReSIS. Trailing antennas have been investigated; however, the beam patterns sample more across-track topography than desirable, increasing cluttering. [1]

C. Directivity Requirements

Directivity is the magnitude of the power density produced by an antenna in the direction which maximizes its value. [2] In this application, it is important that maximum directivity be retained either towards nadir, or in the along-track direction, as in Figure 1. Radiation patterns which sample across-track topography are undesirable as surface scatter increases cluttering, which is manifest in decreased resolution of the synthesized image. [1]

Figure 1. Desirable Along-Track Beam Footprint

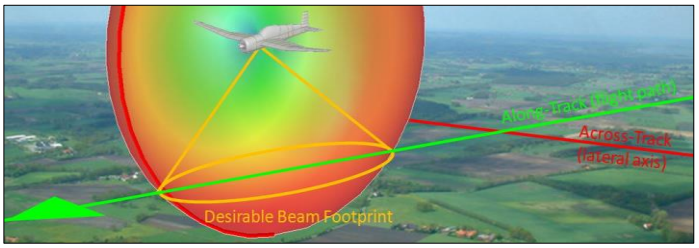

D. Surface-Conformal Implementation

Airborne radar systems and other large antenna systems for aircraft are difficult to design because they must be aerodynamically unobstructive, mechanically secure, and lightweight. Especially in the case of small unmanned aircraft, the drag associated with a protruding antenna element can be considerable and aerodynamically unpredictable depending on the geometry of the components involved.

With the opportunity to implement antenna elements on the surface of the aircraft itself (as is the case with small fiberglass and wood unmanned aerial vehicles), keeping antenna elements conformal to the aircraft was made a design priority. Trailing elements have been problematic in previous versions of the platform. [1]

E. Bandwidth Requirements

Radar systems typically function using a variable frequency RF pulse (commonly a linear frequency "chirp") to illuminate a region of interest, and recording reflections from dielectric boundaries representing topography or variations in density of some material in that region.

Impedance bandwidth is defined as the range of frequency in which the reflection coefficient (Γ_{dB}) exhibited by an antenna or antenna system is lower than -10 dB. [2]

Antennas designed for radar applications need to accommodate the spectrum of the pulses or "chirps" used by that system. Radar specifications for this application necessitate a 10% impedance bandwidth, about the center operating frequencies of 14 MHz and 35 MHz. These minimum bandwidth requirements are 1.4 MHz and 3.5 MHz for the 14 MHz and 35 MHz bands, respectively.

F. Dual-Band Operation

CReSIS is interested in utilizing this platform to collect radar soundings on both the 14 MHz and 35 MHz bands. The aircraft will fly patterns over the area of interest to gather information, and return to a landing site. The ability to collect soundings on both bands without landing to reconfigure antenna elements was made a design priority.

Many antenna designs only exhibit a favorable impedance bandwidth at one frequency. Two electrically separate antennas could be used, but would have to be switched electrically mid-flight to change operating bands, increasing the complexity of the system. Other more geometrically complex antenna designs may respond well at both operating frequencies. [3]

Concepts in both the dual-band single-antenna technique, and the switched dual-antenna technique were investigated for conformity with the design objectives.

G. Background: Previous G1X Unmanned Aerial System

The G1X unmanned aerial system (UAS) has provided CReSIS with a small, maneuverable, and largely non-conductive platform for collecting SAR soundings with HF/VHF antennas and radar equipment. This aircraft is a modified 40% scale Yak-54 aerobatic aircraft. The structure and skin of the aircraft is composed primarily of dielectrics, making implementation of the large antenna elements necessary for HF/VHF radar soundings less challenging.

Extended wings designed at the University of Kansas have been used to increase the original 3.2 meter wingspan to over 5.3 meters, increasing the amount of useable lateral surface for metallization to produce the antenna. The aircraft on approach is visible in figure 2 below.

Figure 2. Previous G1X UAS on approach to land. [1]

This previous platform design utilized two separate antennas, one for each radar band (14 MHz and 35 MHz), visible in Figure 3 below.

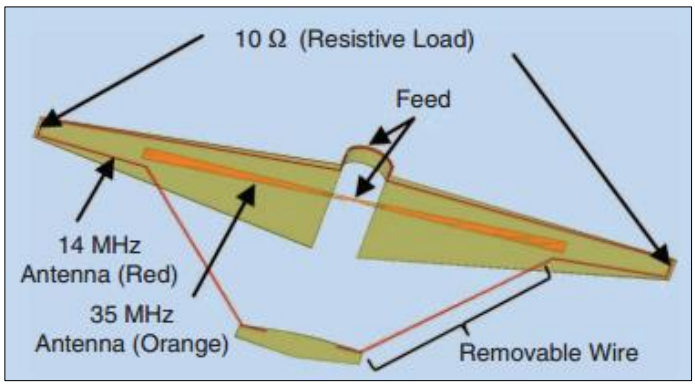

Figure 3. Antenna configuration of the previous G1X Unmanned Aerial System [1]

A wideband bowtie dipole (visible in orange) was used for the 35 MHz band, and an open folded-dipole element (visible in red) was used for the 14 MHz band. [1] The 14 MHz antenna incorporated resistive loading to increase bandwidth, and required trailing antenna elements from the wingtips to the empennage in order to increase the physical length of the antenna and avoid the higher frequency response of a true folded dipole. [3]

In order to change operating frequency, the aircraft needed to land and be serviced to switch antenna feeds and matching networks. [1]

H. G1X-B Unmanned Aerial System

The G1X-B being designed at the time of writing is intended to improve upon results achieved with the G1X. The wingspan is retained with a new and more stable dihedral wing design. Radar equipment is being designed to operate at higher

transmitting power in order to increase resolution and reduce noise.

Aside from upgraded radar equipment and dihedral wings, the airframe is very similar to the original G1X. Figure 4 shows a model of the G1X-B. The design is not finalized at the time of writing, but the outer moldline of the wings has been established.

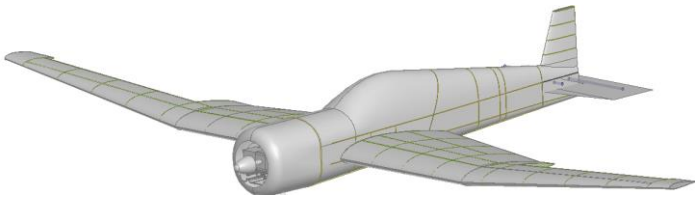

Figure 4. G1X-B airframe model

II. Design

A. Antenna Miniaturization

Despite design considerations to accommodate the large antenna elements necessary, a traditional half-wave 14 MHz dipole would have a length of approximately 10.7 meters, more than twice the wingspan of the aircraft. This design challenge is illustrated in Figure 5 below.

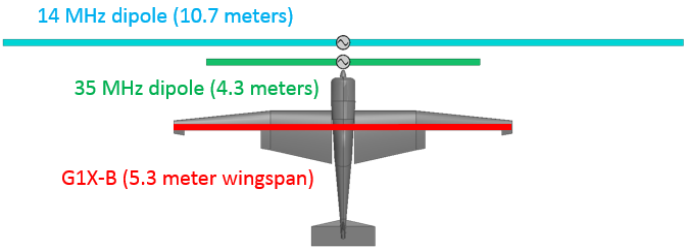

Figure 5. $\frac{1}{2}\lambda$ dipole antenna length and G1X-B wingspan

Antenna miniaturization techniques and small antenna theory are applied almost ubiquitously in mobile electronic devices and communication systems. While most applications operate in the GHz range, the same concepts may be applied to larger antenna systems.

A common miniaturization technique involves modifying antenna geometry or adding lump components to increase the inductive and/or capacitive reactance of the antenna, lowering its resonant frequency. The resulting designs are referred to as slow-wave antennas, as they slow the propagation of electromagnetic waves along the antenna elements. One of the most common slow-wave techniques is meandering, illustrated in Figure 6.

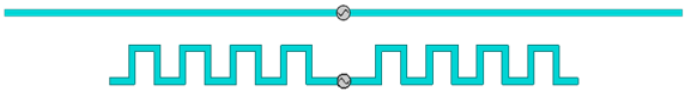

Figure 6. Traditional dipole antenna (top), and approximately electrically equivalent slow-wave dipole, miniaturized by meandering technique (bottom)

Slow-wave antennas, especially of the complex geometry dictated by wing shape and surface conformal design requirement, are difficult to model theoretically. Accordingly, the design process was largely iterative. This process employed high frequency structure simulation software and parametric analyses of different miniaturized antenna geometries in order to arrive at an effective solution.

B. Design Iterations

ANSYS High Frequency Structure Simulator (HFSS) was used to model antenna designs and simulate their performance. The Integral Equations solver (IE solver) was used to decrease simulation time while retaining accuracy, as most conductive geometries involved (copper foils) may be approximated as surfaces.

Suggested designs included both single-antenna dual-band configurations and electrically switched dual-antenna dual-band configurations. The single-antenna configurations provided a simplified design with no mutual coupling to inactive elements, or high-power antenna switching circuitry. However, the dual-antenna designs provided much greater tuning flexibility.

Geometries investigated were based on slow-wave techniques, including different forms of meandering, slotted conductors, normal-mode helical structures, bowtie profiles for increased bandwidth, and dual-element combinations of these structures. Some concepts investigated are visible in Figure 7 below. All of these modeled geometries were parameterized for tuning purposes.

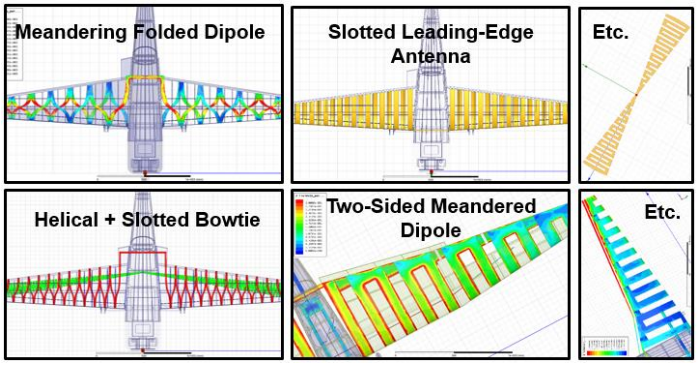

Figure 7. Miniaturized antenna configurations investigated

C. Final Design

Following careful tuning of the most successful single-antenna concept, a design was finalized which could meet the objectives listed previously. This consisted of a meandered element running alternately over the top and bottom surfaces of the wing, as in Figure 8. This design exhibited responses at 14 MHz and 35 MHz which were roughly equal in magnitude. The observed frequency response provided a sufficient starting point for improved bandwidth performance through loading and matching network design.

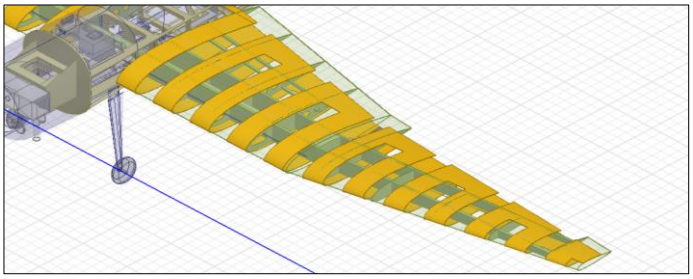

Figure 8. Final antenna design, a folded meandered dipole

Increasing Bandwidth

Slow-wave miniaturization techniques typically involve adding continuous or lumped reactances to an antenna element. This has the effect of electrically lengthening the element, but it also increases the Q factor of the antenna, reducing bandwidth proportionally. In applications with considerable bandwidth requirements, methods for reducing Q factor and increasing bandwidth must be employed.

Radiation efficiency in this application is not as critical a design requirement as bandwidth, with an absolute lower bound of 20%, and ideal lower bound of 40% for relatively efficient radar operation. Through resistive loading, the Q factor of the antenna can be reduced, compromising radiation efficiency for bandwidth. Loading of 30 Ω series resistance per antenna element was used, lowering radiation efficiency to 45% and 35% for the 14 MHz and 35 MHz bands, respectively.

Placement of these resistive elements along the conductor is another tuning parameter, and can be used to adjust the bandwidth and radiation efficiency of either operating band independently. Figure 9 demonstrates resistor placement which provided acceptable bandwidth performance at both frequencies. (See Figure 10 for frequency response).

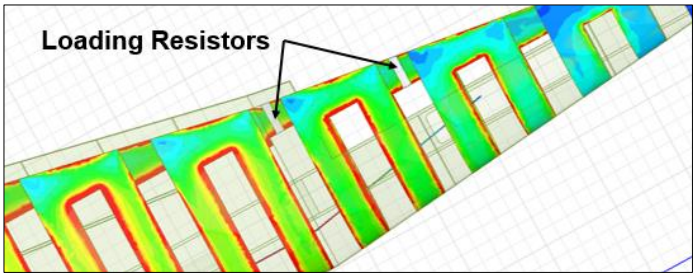

Figure 9. Loading resistor placement (15 Ω each)
(Note simulated current density on the conductors)

D. Simulated Response

The final frequency response of this single-antenna dual-band design with optimized loading for increased bandwidth is visible in Figure 9 below, along with surface charge and lateral-vertical plane radiation patterns on both the 14 MHz (Figure 10) and 35 MHz (Figure 11) operating bands.

Figure 9. Dual-Band Frequency Response

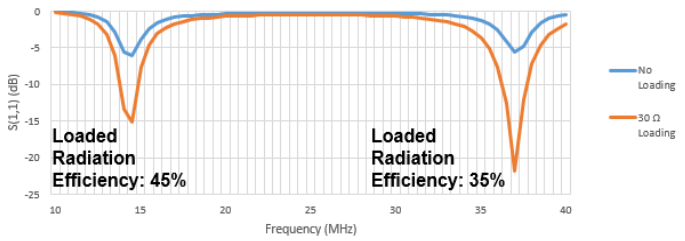

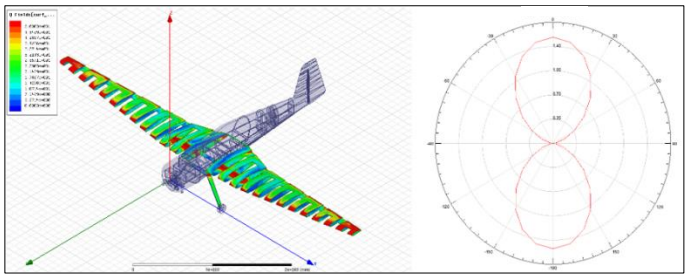

Figure 10. Simulated surface charge and radiation pattern plots for the 14 MHz band.

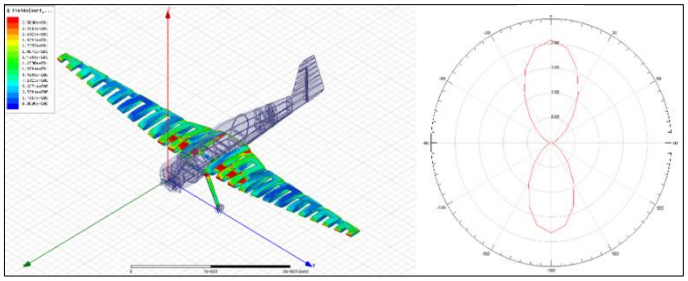

Figure 11. Simulated surface charge and radiation pattern plots for the 35 MHz band.

The beam patterns in the lateral-vertical plane (Figures 10 and 11) fit directivity requirements, particularly in the case of the 35 MHz band. However, with a large mismatch between antenna impedance and simulated port impedance, bandwidth is not optimized.

E. Matching Network

In order to match antenna impedance (below 50 Ω, and different for both operating bands) to transmission line impedance (50 Ω), the reflection coefficient frequency response was imported into Keysight Genesys RF design software. A high-order bandpass matching network was optimized to achieve the established 10% impedance bandwidth requirements on both operating bands, in order to demonstrate that the antenna could be made to meet the established design objectives. See Figure 12 for matching network optimization results.

The matching network used was a 10th order bandpass network requiring 21 components. However careful optimization could significantly reduce the order and number of parts required for a match.

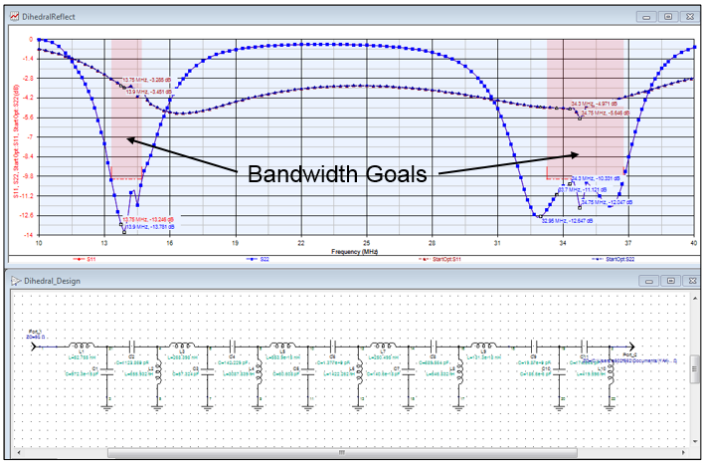

Figure 12. Matching network used to achieve target bandwidths

III. SCALE PRODUCTION & TESTING

A. Scale Testing Motivations

The results obtained through simulation in HFSS appear to satisfy design criteria; however, in order to verify the simulated results, a scale model was produced. This is also necessary to ensure that the design is feasible to implement.

The scale model will be analyzed in the Electromagnetic Anechoic Chamber at the University of Kansas, therefore a scale of 15% was used, such that the maximum model size (800mm), scale center frequencies ($F_{15\%}$ = 93 MHz scale for 14 MHz band, and $F_{15\%}$ = 233 MHz scale for 35 MHz band), and scale wavelengths ($\lambda_{15\%}$ = 3.2m scale for 14 MHz band, and $\lambda_{15\%}$ = 1.3m scale for 35 MHz band) fit criteria for far-field measurement given chamber dimensions.

B. Scale Wing Production

Autodesk Inventor was used to finish and thicken the wingskin model for production via 3D printing from High Impact Polystyrene (HIPs). Inboard ribs were approximated by a single filled region in order to accommodate the 3D printing process.

The full-sized wings contain an insignificant volume of dielectric material. This property had to be retained in the scale model. Fill settings, which define structure automatically placed inside an object by 3D printing software, were minimized, and the outboard wing sections were made hollow. Inboard and outboard wing sections were produced to fit the printer's build volume (Figure 13) and glued together to form the finished wing, as in Figure 15.

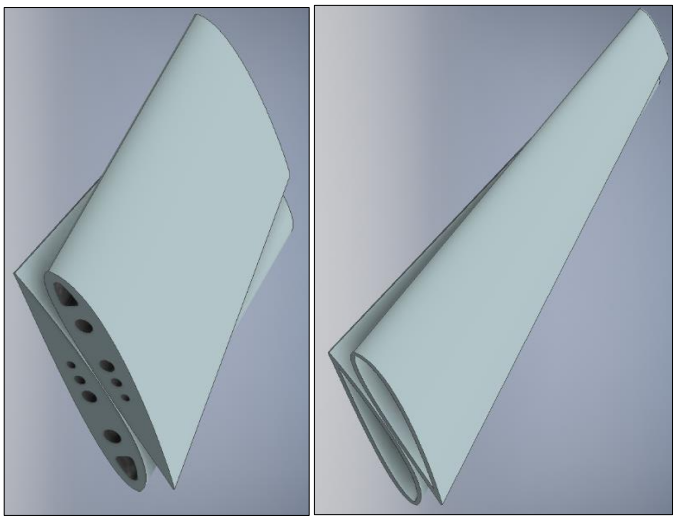

Figure 13. Inboard (right) and outboard (left) mirrored wing sections prepared for production via 3D printing

C. Antenna Pattern Production

The antenna design was exported from HFSS as a surface, and Rhinoceros 3D modeling software was used to unfold the developable surface into a pattern, as in Figure 14.

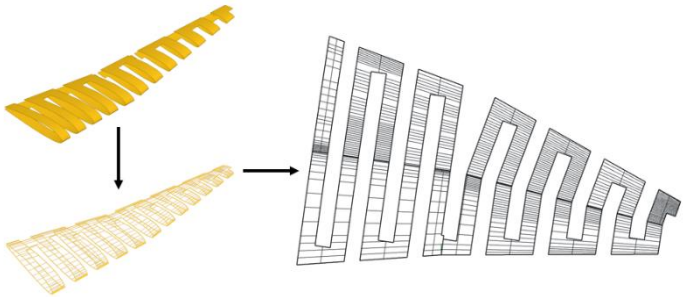

Figure 14. Unfolding process yielding flat conductor pattern

D. Model Construction

The antenna element patterns were used to cut adhesive-backed copper foil and produce the scale antenna elements. These were carefully applied to the finished wing as in Figure 15.

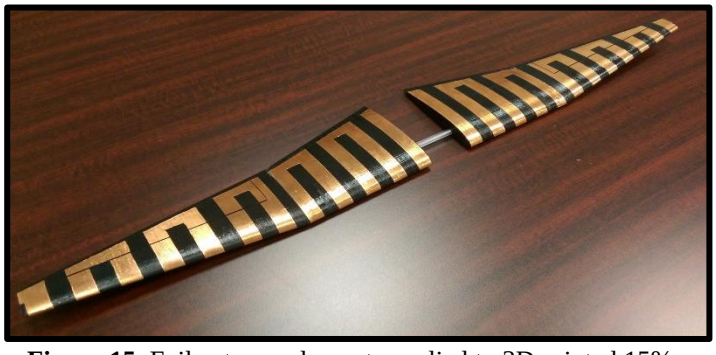

Figure 15. Foil antenna elements applied to 3D printed 15% scale G1X-B wing model

Slots were cut in the elements, representing longitudinal separations caused by the control surface, as in Figure 16. To simulate the lump resistances added, 15Ω 1205 surface mount resistors were soldered in series with the antenna elements, as in the simulations.

Simulated current density overlays were used to determine component placement such that the component intersects the conductor where current density is maximized, as in Figure 9. Accordingly, the resistors were positioned toward the inside of the wing, as in Figure 16.

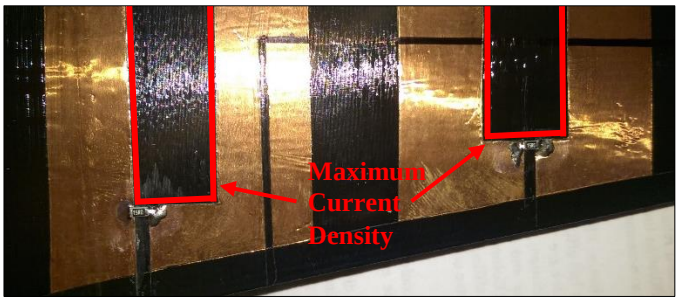

Figure 16. Resistor placement to intersect maximum current density in the conductor

Because the antenna is a symmetrical dipole being driven by an unbalanced coaxial transmission line, the antenna feed needed to incorporate a balun.

A Coilcraft PWB-1-AL 1:1 surface mount wideband RF transformer, with rated attenuation < 2dB from 13 KHz to 350 MHz, was used to implement a Guanella-type current balun. The balun was connected directly to an edge-mount SMA connector, and to the antenna feed, as in Figure 17.

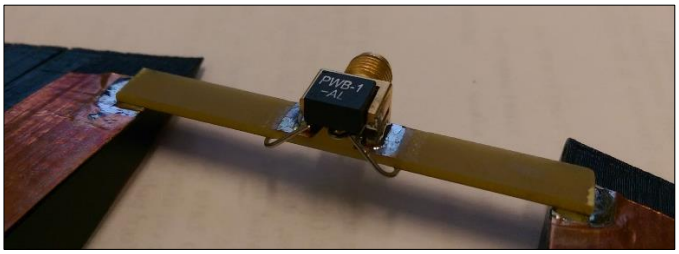

Figure 17. Antenna feed with Guanella-type current balun

E. Testing Procedure

The scale antenna system was analyzed in the University of Kansas Electromagnetic Anechoic Chamber. The antenna was mounted horizontally via nonconductive tripod on a theta turntable in the chamber such that the horizontally-polarized reference antenna sampled the lateral-vertical plane with respect to the aircraft (see Figure 18).

Figure 18. Antenna positioned in the anechoic chamber for testing.

A network analyzer was used to measure the frequency response of the antenna in terms of reflection coefficient.

To collect radiation patterns, a second port was connected to the horizontally-polarized reference antenna, and control software was used to rotate the theta turntable and collect an E-plane cut at both scale frequencies of 93 MHz and 233 MHz.

F. Scale Testing Results

The scale antenna system performed as expected, given simulation results. Frequency response was comparable, with a slight downward shift. An increase in loss, manifest in increased apparent bandwidth and lower reflection coefficient peaks, was apparent and is visible in Figure 19.

These effects are likely a product of the disproportionate dielectric thickness used to represent the wingskin in the model, which was 3mm of High-Impact Polystyrene. The skin of the model was required to be substantial in order for the part to remain durable. However, this misrepresents the skin thickness of the full-scale aircraft, which will only a few millimeters, and should be electrostatically negligible.

This volume of thermoplastic dielectric was not simulated, therefore the resulting increased capacitive reactance of the antenna and dielectric loss can explain the deviation in frequency and magnitude, respectively, of the measured scale results.

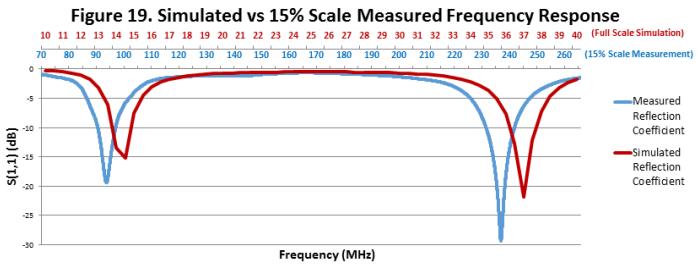

Radiation patterns, in the form of E-plane cuts in the lateral-vertical axis with respect to the aircraft, were collected and normalized. These compare very closely with the simulated patterns at both 14 MHz (93 MHz scale) and 35 MHz (233 MHz scale). These plots are visible in Figure 20 and Figure 21, respectively.

Figure 20.

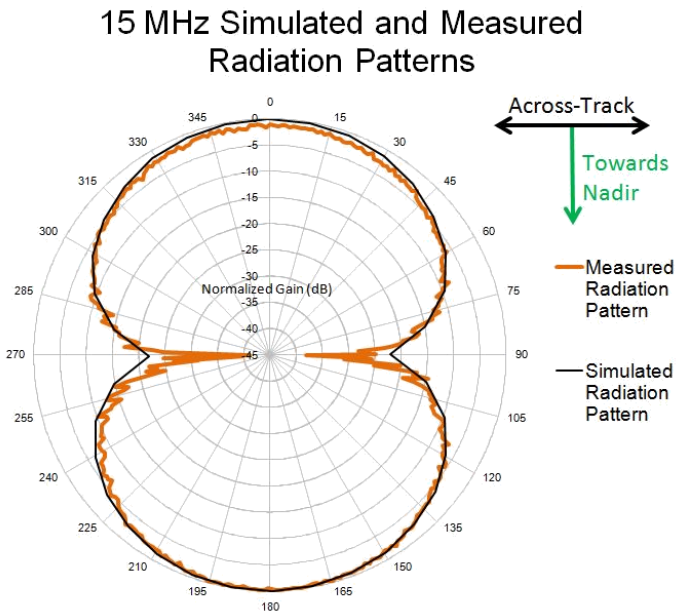

Figure 21.

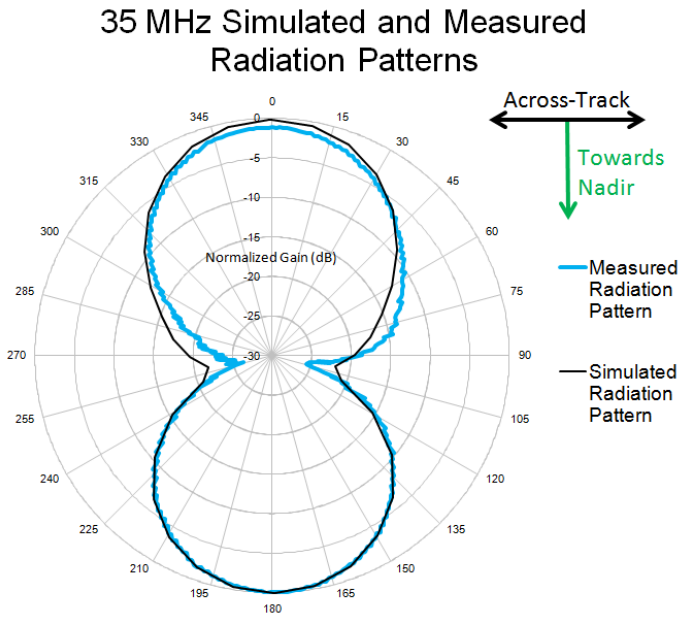

Further investigation might include simulating the dielectric wingskin thickness of the model in order to more completely reconcile simulated results with scale testing results of different antenna configurations.

IV. CONSIDERATIONS FOR IMPLEMENTATION

A key design consideration was ease and practicality of implementation on the full-scale aircraft. Considerations need to be made in order to allow for the most effective antenna design, while retaining the utility and performance of the platform.

A) Electrical Utilization of Control Surfaces

Control surfaces (in this case, the ailerons of the G1X-B) account for much of the valuable wing surface available for metallization to produce the antenna. Utilization of these surfaces is critical to the implementation of an effective antenna. A method for electrically connecting wing-based antenna elements to control surface-based elements must then be proposed.

The connection needs to remain aerodynamically and mechanically unobstructive. Flexible Printed Circuit (FPC) comprised of thin conductors laminated in polyamide film, are ubiquitous in the electronics industry for making low-profile flexible electrical connections. The connectors associated with these FPC cables can have a vertical profile of less than two millimeters, and would be used to facilitate the replacement of fatigued jumpers.

A model of the interface between the wing and aileron of the G1X-B was produced using balsa wood metalized with copper foil, and used to test different FPC based jumper configurations, as in Figure 22. These connections do not affect the actuation of the control surface as modeled and appear to avoid creasing and excessive fatigue when routed carefully.

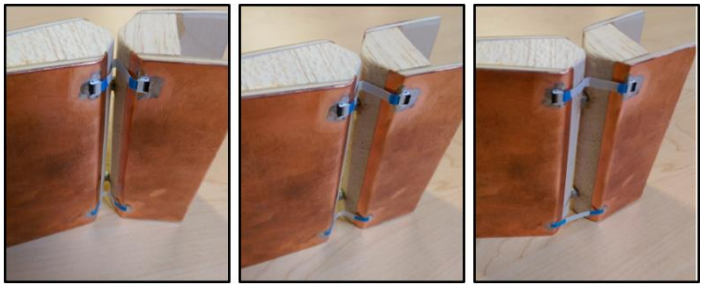

Figure 22. Actuation of the modeled FPC electrical connections at the aileron-wing interface of the G1X-B

B) Sensitivity to Internal Conductors

A drawback of the single-antenna dual-band design is the sensitivity of the meandered antenna to detuning by nearby conductors. These conductors couple capacitively with the meandered elements, providing a shorter electrical path from element to element, muting and distorting the frequency response attained through meandering.

With conductive elements inside the wing unavoidable, this must be addressed.

Servo Wires

Running most of the length of the wing to servos actuating the outboard aileron, these wires provide opportunities to reduce interaction through careful routing and the production of air-core inductive elements at any point within the wing. These coils can be used to separate what would otherwise be a continuous conductor through the entire wing into smaller sections that can't share current easily at the antenna's operating frequency due to the impedance of the coils.

Main Spar

The main spar of an aircraft such as the G1X-B is responsible for carrying flight loads and is therefore a critical structural element. The spar runs through the fuselage and inboard wing sections. Materials commonly used are fiberglass and carbon fiber composites.

Fiberglass is not conductive, and does not present a problem. Carbon fiber, however, conducts along the direction of the weave. The unidirectional carbon fiber patterns used to produce spars that handle bending loads and normal stresses will conduct along their length. These spars are also incredibly lightweight and attractive in aerospace applications. The geometry of the spar cannot be modified, so accommodations must be made in the form of modified antenna geometry in order to avoid electromagnetic interaction.

V. Conclusions and Further Queries

This antenna design represents a simple and effective dual-band solution for the G1X-B UAS, allowing for the collection of soundings on multiple radar bands without modification or electrical switching. Simulated response and radiation patterns correspond very closely with those modeled in scale, with any discrepancies easily explained by the structure of the model.

Pending investigation are issues related to servo wire routing, accommodation of a carbon fiber spar, the design and testing of a physical matching network, and refinement of the FPC method for electrically incorporating aileron surface as part of the antenna element.

Acknowledgment

I would like to thank Dr. Yan for his superb mentorship and support through the course of the project. His expertise and intuition made this work possible, and I am lucky to have had the opportunity to be part of the team. Dr. Rodriguez-Morales provided valuable insight into the operation of the radar system and advice for constructing testing apparatus.

Graduate research assistant Ali Mahmood, who designed the antenna system for the previous G1X, provided a wealth of background information about the project, as well as advice and suggestions for possible designs.

Graduate student Katie Constant and her advisor Dr. Hale from the Aerospace Engineering Department at KU gave valuable input regarding the limitations of the airframe and the specifics of the design of the aircraft. Close communication with aerospace faculty has proven critical in producing a feasible design which is easy and unobstructive to implement.

Dave Dalton, owner of the Hammerspace Community Workshop in Kansas City, assisted in contacting Tom Newell, owner of Oni Technology LLC, the 3D-printing company contracted with producing the G1X-B 15% scale wings. Without Dave and Tom's hard work, CReSIS would be without a valuable tool for evaluating future designs.

Lastly I would like to thank Education Coordinator Darryl Monteau for her close work with the REU program and its students, and for making our time with CReSIS such a memorable and valuable experience.

References

[1] . Leuschen, C., Hale, R., Keshmiri, S., Yan, J., Rodriguez-Morales, F., Mahmood, A., & Gogineni, S. (n.d.). UAS-Based Radar Sounding of the Polar Ice Sheets. IEEE Geosci. Remote Sens. Mag. IEEE Geoscience and Remote Sensing Magazine, 8-17.

[2] Volakis, J. (2007). Antenna Engineering Handbook (4th ed.). New York City, New York: McGraw-Hill.

[3] Volakis, J., Chen, C., & Fujimoto, K. (2010). Small antennas: Miniaturization techniques & applications. New York: McGraw-Hill.